Published by
NIGERIAN SOCIETY OF PHYSICAL SCIENCES
Available online @ https://journal.nsps.org.ng/index.php/jnsps

J. Nig. Soc. Phys. Sci. 4 (2022) 214–222

Journal of the Nigerian Society of Physical Sciences

The corrosion characteristics of SS316L stainless steel in a typical acid cleaning solution and its inhibition by 1-benzylimidazole: Weight loss, electrochemical and SEM characterizations

K. K. Adama[a], I. B. Onyeachu[b,*]

[a] *Department of Chemical Engineering, Faculty of Engineering, Edo State University Uzairue, Edo State, Nigeria.*
[b] *Department of Industrial Chemistry, Faculty of Science, Edo State University Uzairue, Edo State, Nigeria.*

Abstract

Acid cleaning, an inevitable industrial practice used to descale chemical reactors, usually causes serious corrosion attack on underlying alloy substrates. Ameliorating this phenomenon requires the addition of effective corrosion inhibitors into the acid solution. Current global regulations encourage environmentally-benign molecules as corrosion inhibitors. Consequently, 1-benzylimidazole has been investigated for its inhibitive characteristics against the corrosion of SS316L stainless steel in a typical acid cleaning solution containing 2 % HCl + 3.5 % NaCl. Weight loss measurements confirm that the corrosion inhibition property of 1-benzylimidazole increases with concentration but depreciates with increased temperature. Electrochemical impedance spectroscopy (EIS) and potentiodynamic polarization (PDP) measurements confirm that 1-benzylimidazole adsorb on the stainless steel surface to isolate its surface from the acid solution. 1-benzylimidazole is a mixed-type inhibitor with greater anodic influence, and its adsorption enhances the formation and protectiveness of a passive film. Weight loss and the electrochemical measurements agree to an average inhibition efficiency > 70 % at 1000 ppm. The inhibitor adsorbs via physisorption and obeys the Temkin isotherm model. SEM surface characterization confirm the ability of 1-benzylimidazole to protect the surface microstructure of the stainless steel during the corrosion.

DOI:10.46481/jnsps.2022.596

Keywords: Corrosion inhibitor; Stainless steel; Acid cleaning; Imidazole; Polarization.

Article History :
Received: 18 January 2022
Received in revised form: 17 March 2022
Accepted for publication: 19 March 2022
Published: 29 May 2022

Communicated by: Edward Anand Emile

1. Introduction

Stainless steel is heavily deployed in the construction of many reactors in the chemical industry. It exhibits good corrosion resistance because it readily forms an iron/chromium-enriched passive layer [1]. Unfortunately, the passive film formation is usually truncated by chloride ion-containing corrosion environments because its products are transformed into soluble chlorides [2]. The resultant effect is a localized form of corrosion which diminishes the structural integrity of many chemical reactors and shortens their span of usage. Acid cleaning is a typical industrial process which exposes stainless steel surfaces to chloride ion-induced corrosion. It involves the use of dilute mineral acid (especially 2-5 % HCl) to remove inorganic scales which grow on the surfaces of industrial

*Corresponding author tel. no: +2348034917997
Email address: onyeachu.benedict@edouniversity.edu.ng (I. B. Onyeachu)

metallic equipment and diminish their performance. While the metal surface is descaled, a simultaneous acid corrosion attack on the underlying substrate usually ensues. The extent of this corrosion is even aggravated by the seawater sources used to prepare the acid solutions, since seawater is naturally enriched with chloride ions, especially as NaCl [3, 4]. A practical industrial approach to ameliorate this corrosion attack is to add highly effective corrosion inhibitors into the acid cleaning solution. Currently, most industries apply propargyl alcohol-based inhibitors which are very toxic, both, to humans and other environmental species [5].

Imidazole and its derivatives are nitrogen-based heterocyclic compounds largely used for the production of numerous cheap environmentally-safe drugs [6, 7]. In the past decade, imidazole derivatives have been reported as formidable corrosion inhibitors for various metals. Singh et al. [8] reported that 2-(4-methoxyphenyl)-4,5-diphenyl-imidazole exhibited 93 % efficiency for the inhibition of J55 steel corrosion in CO_2-saturated brine solution. Ting et al. [9] reported that 4-phenylimidazole acted as a mixed-type corrosion inhibitor for copper in sulphuric acid and provided 95.84 % efficiency; adsorbing both by physical and chemical mechanisms. In other reports [10], thiazole-4-carboxylic acid, 2-methyl-1,3-thiazole-4-carboxylic acid, and some imidazole zwitterions have been reported as highly efficient for carbon steel during acid corrosion [11]. Particularly, dimethylbenzodiimidazole (2,7-dimethyl3,6-dihydrobenzo[1,2-d;3,4-d'] diimidazole acted as an anodic inhibitor for SS316L stainless steel in 0.5 M H_2SO_4 and provided 77 % at optimum concentration [12]. Also, some synthesized dicationic imidazolium ionic liquids were also reported for SS304 stainless steel in 0.5 M H_2SO_4 solution whereby 92 % efficiency was recorded [13]. Apparently, not much work has been reported for imidazole derivatives as stainless steel corrosion inhibitors. Even so, the reported derivatives are expensively synthesized compounds with cumbersome molecular structures that disturb their adsorption. Identifying a cheap and simple-structure imidazole derivative which can deliver high inhibition efficiency will be very beneficial to the industry.

In the present work, 1-benzylimidazole has been identified as a promising imidazole derivative for the inhibition of stainless steel acid corrosion. 1-benzylimidazole is a major pharmacological ingredient with environmentally-safe characteristics, according to the Paris Commission (PARCOM) standard [14], because it exhibits $\log P_{o/w}$ = 1.93 and LD_{50} = 75 mg/kg [15]. As Figure 1 shows, 1-benzylimidazole has a simple structure whereby a phenylmethyl group is attached to the imidazole nitrogen. Computational simulation previously revealed that this simple structure enables 1-benzylimidazole to inherently orient in a flat position and achieve good metal surface coverage during corrosion inhibition [16]. The most visible reports of 1-benzylimidazole as corrosion inhibitor have been presented for carbon steel [16, 17, 18] in acid solutions. The inhibitor exhibited more anodic behaviour on the carbon steels, causing us to suspect its ability to enhance anodic passivation when applied for stainless steel. Furthermore, the inhibitor efficiency has not been reported in a practical acid cleaning solution which contains HCl + NaCl, and is usually conducted at elevated temperatures [3]. Filling this research gap will be highly beneficial towards the development of greener corrosion inhibitors for industrial acid cleaning.

Consequently, we apply weight loss technique to screen the effect of concentration and temperature on the performance of 1-benzylimidazole as inhibitor against the corrosion of SS316L stainless steel in 2 % HCl + 3.5 % NaCl solution. Thereafter, we employ electrochemical techniques like electrochemical impedance spectroscopy (EIS) and potentiodynamic polarization (PDP) to provide mechanistic interpretation of 1-benzylimidazole performance at maximum concentration. Scanning electron microscopy (SEM) was employed to probe the extent of stainless steel surface damage by corrosion and its mitigation by the 1-benzylimidazole.

2. Materials and method

2.1. Materials

All chemicals and reagents used in this work were purchased from Sigma Aldrich and Fischer Scientific, respectively. Stainless steel SS316L, having the elemental composition previously reported [19], was used. The bulk alloy bar was machined into corrosion test coupons with total surface area 24.89 cm^2 and 1 cm^2 , respectively, exposed for the weight loss and electrochemical experiments. The test solution (2 % HCl + 3.5 % NaCl) was prepared by, firstly, diluting concentrated HCl (37 w/v%) with distilled water to obtain a 2 % HCl solution and, secondly, preparing 3.5 % NaCl solution using the 2 % HCl as solvent. Stock solution of 1-benzylimidazole was prepared in isopropanol and calculated volumes were subsequently retrieved and made up to 200 mL with the acid solution, so as to obtain working inhibitor concentrations of 200, 400, 800 and 1000 ppm. A thermostatic water bath was employed to maintain experimental temperatures.

2.2. Methods

Prior to any experiment, the surface of the stainless steel coupon was polished with #400, #600, #800 and #1000 grit silicon carbide papers. This was performed with simultaneous washing under running tap water, degreasing with acetone and mechanical drying with warm air. Weight loss experiments, after 24 h immersion in the uninhibited and inhibited acid solutions, were conducted, initially, at 25°C. Using the optimum inhibitor concentration, the effect of temperature (45 and 65°C) was investigated. The stainless steel coupons were retrieved after 24 h immersion and cleaned according to the ASTM G1-03 standard procedure [20]. The coupons were then re-weighed and the weight difference (ΔW) before and after immersion was calculated based on Equation (1). From the weight loss, the corrosion rate (CR) in millimeter per year (mpy) was calculated, based on Equation (2); where A = total surface area of coupon

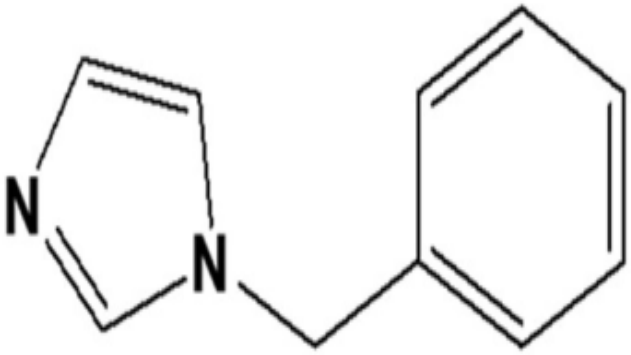

Figure 1: Structure of 1-benzylimidazole.

(24.89 cm^2), ρ = density of SS316L stainless steel (8.0 g cm^{-3}), T = immersion time (24 h).

$$\Delta W = W_{\text{before}} - W_{\text{after}} \tag{1}$$

$$CR(mpy) = \frac{\Delta W \times 3.45 \times 10^6}{A \times \rho \times T} \tag{2}$$

The electrochemical experiments such as EIS and PDP were conducted on a Gamry 600 potentiostat equipped with the Echem Analyst software for data analysis. The electrochemical set-up was a 3-electrode system which contained the stainless steel as the working electrode, a graphite rod as counter electrode and Ag/AgCl as the reference electrode. All measurements were performed at the end of 1 hour free immersion to ensure that the corrosion coupons attained steady-state open circuit potential [21]. The EIS measurement was conducted by applying ± 10 mV sinusoidal signal amplitude perturbation over a frequency range of 10^5 Hz to 10^{-1} Hz. The PDP experiment was conducted by polarizing the stainless steel from −0.25 V (vs. open circuit potential) to +1.2 V vs. Ref. at a rate of 0.2 mV/s . The SEM surface characterization for the polarized inhibited and uninhibited electrode was achieved using the JEOL JSM-6610 LV scanning electron microscope.

3. Results and discussion

3.1. Weight loss results

The weight loss, and associated corrosion rate, experienced after 24 h immersion of the stainless steel coupons in 2 % HCl + 3.5 % NaCl solution at 25°C without and with different 1-benzylimidazole concentrations are presented in Figures 2a and 2b. In the acid solution without inhibitor, the stainless steel loses an average of 0.0411 g after 24 h immersion, which corresponds to a corrosion rate of 30.20 mpy. In the presence of 1-benzylimidazole, the weight loss diminishes continually with increasing inhibitor concentration. The least average weight loss of 0.0109 g (or 8.01 mpy corrosion rate) was observed in the presence of 1000 ppm, and approximated to 73.48 %, following Equation (3) and Figure 2c.

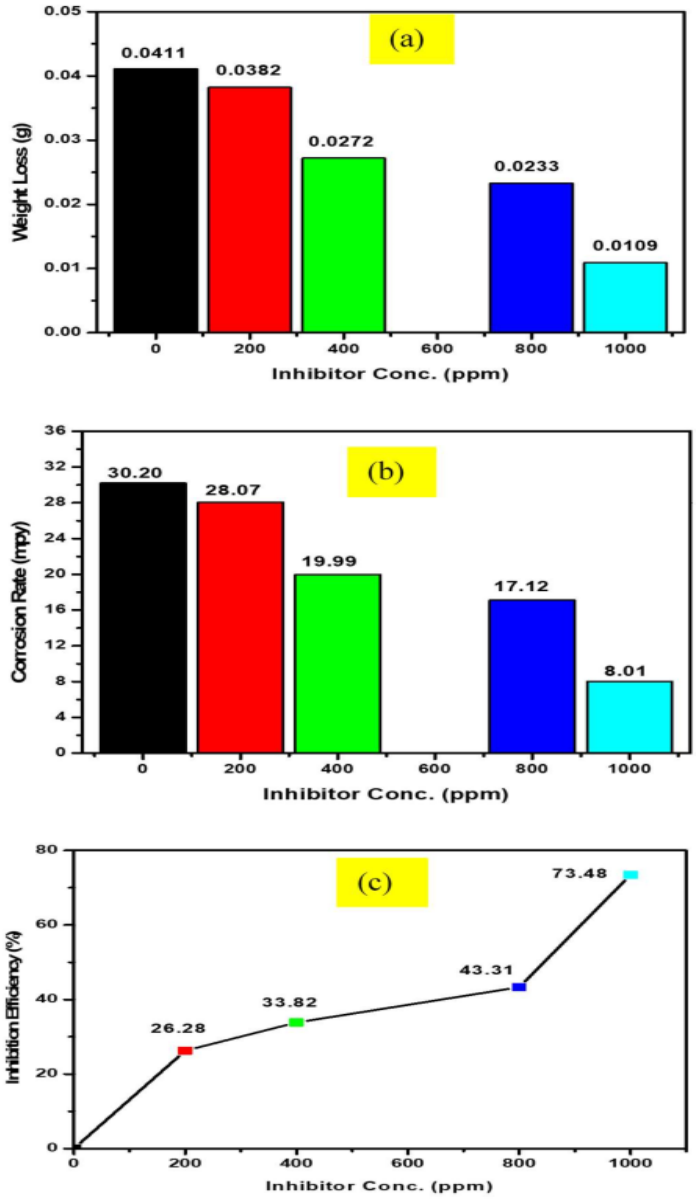

Figure 2: Results of (a) weight loss (b) corrosion rate and (c) inhibition efficiency after 24 immersion of SS316L stainless steel in 2 % HCl + 3.5 % NaCl solution without and with different concentration of 1-benzylimidazole at 25°C

$$\%IE_{\Delta W} = 1 - \frac{CR_{\text{with inhibitor}}}{CR_{\text{without inhibitor}}} \times 100\% \tag{3}$$

This result can be interpreted by considering that the weight loss experienced by the immersed coupons is caused by the loss of surface atoms like Cr and Fe via oxidation into species like Cr^{3+} , Fe^{2+} and Fe^{3+}. On the other hand, organic inhibitors impede corrosion by interacting the reactive electrons n their heteroatoms and $C = C$ functional groups with the d-orbitals of metal atoms. These electron-rich sites donate electrons that fill the d-orbitals in the metal atoms, thus, supressing their oxidation. The resultant inhibitor adsorption increases the hydrophobicity of the metal surface and isolates it from the corrosion environment, as the schematic in Figure 3 elucidates. The more inhibitor in the acid solution, the more metal surface

is covered and protected.

As temperature increases to 45 and 65°C, Table 1 shows that the weight loss and corrosion rate increase for, both, the uninhibited and inhibited acid solutions. The corrosion inhibition efficiency provided by the maximum concentration of 1000 ppm, initially, decreased rather moderately to 67.80 % (45°C) and, thereafter, quite drastically to 37.61 % (65°C). Although the presence of 1-benzylimidazole, somewhat, protected the stainless steel at these elevated temperatures, the depreciation in inhibitor efficiency may be attributed to the competitive mechanisms of increased surface dissolution and weakened inhibitor adsorption. Increased temperature promotes the transfer of corrosive agents, especially the chloride ions, from solution bulk to the metal surface, thus, promoting surface dissolution rather than inhibitor adsorption. Also, elevated temperatures could induce desorption of already adsorbed inhibitors from the metal surface, indicating that 1-benzylimidazole adsorbs via a physiosorption mechanism [22].

3.2. Adsorption isotherm

Adsorption isotherms provide adequate understanding of the mode of interaction between an adsorbing corrosion inhibitor molecule and the metal substrate. They describe whether inhibitor molecules adsorb on the metal surface as a single layer of film, as multilayer, or if any repulsion exists among inhibitor molecules [23]. In this research, the Langmuir, Temkin and Freundlich isotherms were employed to test the mode of interaction of 1-benzylimidazole on the stainless steel surface. The Langmuir isotherm predicts that the inhibitor adsorbs on the stainless steel surface as a monolayer. The Temkin isotherm predicts that the inhibitor forms a multilayer with plausible inhibitor-inhibitor interaction. On the other hand, the Freundlich isotherm depicts that the inhibitor is adsorbing on a rough and heterogeneous surface. The linear forms of the Langmuir, Temkin and Freundlich isotherms are, respectively, presented as follows:

$$\frac{C}{\theta} = \frac{1}{K_{ads}} + C \tag{4}$$

$$\theta = -\frac{1}{2\alpha}\ln C - \frac{1}{2\alpha}K_{ads} \tag{5}$$

$$\log\theta = \log K_{ads} + \frac{1}{n}\log C \tag{6}$$

θ = surface coverage = $\frac{\%IE}{100}$, K_{ads} = adsorption-desorption equilibrium constant, C = inhibitor concentration (in ppm) and the factor, α, accounts for the lateral interaction between inhibitor and metal surface.

The value of n describes the feasibility of inhibitor adsorption; which is highly feasible when $0 < \frac{1}{n} < 1$ but, respectively, moderate or difficult when $\frac{1}{n} = 1$ or > 1 [24]. A plot of versus C will yield the Langmuir isotherm curve, as shown in Figure 4a. The Temkin isotherm, Figure 4b, is described by the plot of θ against $\ln C$ whereas the plot of $\log\theta$ versus $\log C$ gives the Freundlich isotherm, Figure 4c. Given that it displayed the closest agreement between experimental plots and fitting line, and because its correlation coefficient (R^2) value was closest to unity, the Freundlich isotherm most appropriately describes the adsorption of 1-benzylimidazole on the SS316L stainless steel. The adsorption equilibrium constant was calculated as 1.025 ppm mol^{-1} and, from this value, the Gibbs' free energy ($\Delta G_{ads} = -RT\ln(10^6 K_{ads})$) was deduced as -34.29 kJ/mol and the negative value of ΔG confirms that the inhibitor adsorption was spontaneous and feasible.

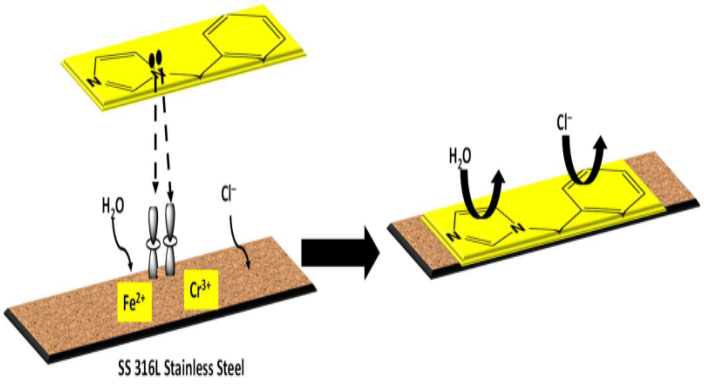

Figure 3: Schematic representation to show how 1-benzylimidazole adsorption increases the hydrophobicity of the stainless steel surface

3.3. Electrochemical results

Electrochemical measurements are capable of providing mechanistic explanations to the corrosion inhibition behaviour of 1-benzylimidazole on the SS316L stainless steel in the acid solution. At the open circuit potential, a quasi-equilibrium is established between the rates of oxidation and reduction reactions taking place in the micro-cells forming anodic and cathodic active sites on the alloy surface. By displacing the alloy from its equilibrium potential, relevant electrochemical parameters could be measured and related to the corrosion phenomenon. Steady-state electrochemical techniques like EIS can provide accurate information about the dielectric and charge transfer phenomena at the alloy-acid solution interface. A more aggressive technique like the PDP is able to provide details about the corrosion potential, corrosion kinetics, passivation and passivation breakdown/pitting corrosion phenomena.

The EIS results are presented in Figure 5, as the plots of Nyquist (Figure 5a), absolute impedance (Figure 5b) and phase angle (Figure 5c). The characteristic arcs displayed by the stainless steel appear larger in the presence of 1-benzylimidazole, compared with the size in the blank acid solution. Larger arcs usually depict greater resistance to charge transfer at the alloy-solution interface, i.e. greater corrosion resistance. The result confirms the inhibitive property of 1-benzylimidazole for the stainless steel. The trend in the Nyquist arc sizes is confirmed by the values of low-frequency absolute impedance in Figure 5b. Clearer mechanism is

Table 1: Weight loss, corrosion rate and inhibition efficiency of 316 stainless steel during corrosion after 24 h in 2 % HCl + 3.5 % NaCl solution at 25°C, 45°C and 65°C

Parameter	25°C		45°C		65°C	
	Weight loss (g)	Corrosion rate (mpy)	Weight loss (g)	Corrosion rate (mpy)	Weight loss (g)	Corrosion rate (mpy)
Without inhibitor	0.041 g	30.20 mpy	0.059 g	43.35 mpy	0.109 g	80.71 mpy
with 1000 rpm	0.011 g	8.01 mpy	0.019 g	13.96 mpy	0.068 g	50.35 mpy
Inhibition Efficiency (% IE)	73.48 %		67.80 %		37.61 %	

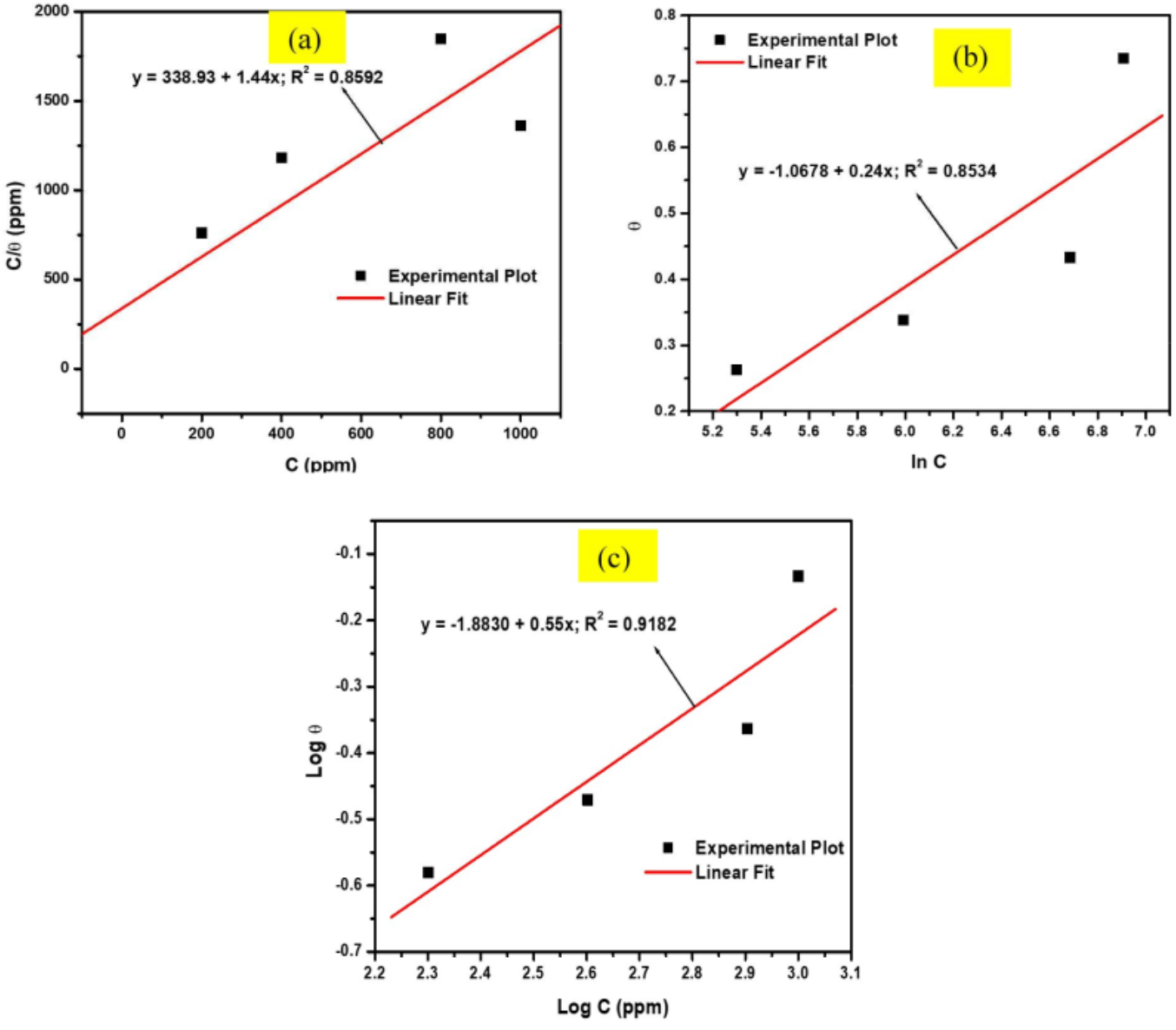

Figure 4: (a) Langmuir (b) Temkin and (c) Freundlich isotherm plots for the adsorption of 1-Benzylimidazole on 316 stainless steel during corrosion in 2 % HCl +3.5 wt% NaCl solution

deduced from the phase angle plots in Figure 5c, whereby the stainless steel clearly displayed two time constants at high and low frequencies, compared with the single time constant exhibited by the uninhibited alloy. The two time constants depict two phenomena at the alloy-solution interface; namely the phenomenon at a corrosion layer-solution interface (at high

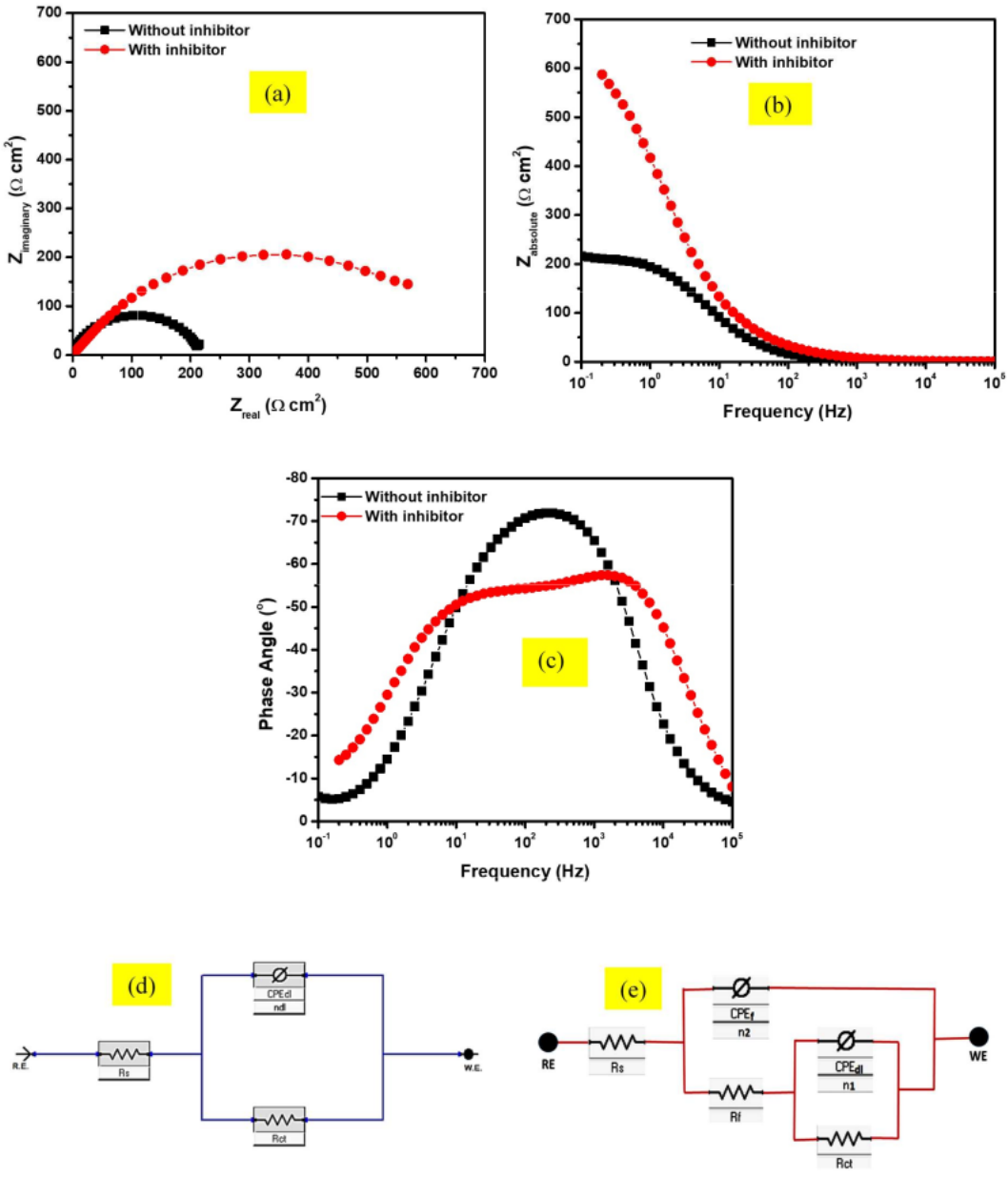

Figure 5: EIS plots in formats of (a) Nyquist (b) absolute impedance (c) phase angle and equivalent circuit for SS316L stainless steel during corrosion in 2 % HCl + 3.5 % NaCl (d) without and (e) with 1-benzylimidazole.

Table 2: EIS parameters for corrosion of 316 stainless steel in 2 % HCl + 3.5 % NaCl solution without and with 1000 ppm of 1-benzylimidazole at 25°C.

	CPE_{dl}				CPE_f					
Conc.	R_s (Ωcm^2)	Y_{dl} $\mu F cm^{-2} s^{n-1}$	α_{dl}	R_{ct} (Ωcm^2)	Y_f $\mu F cm^{-2} sn^{-1}$	α_f	R_f (Ωcm^2)	$(R_p = R_f + R_{ct})$ (Ωcm^2)	Goodness of fit $(\times 10^{-3})$	% IE
without inhibitor	0.719	374	0.75	212	-	-	-	212	3.92	-
with 1000 rpm	0.877	110	0.85	685	57	0.83	80	765	2.29	72.29

Table 3: Polarization parameters for corrosion of 316 stainless steel in 2 % HCl 3.5 % NaCl solution without and with 1000 ppm of 1-benzylimidazole at 25°C.

Sample	E_{corr} (mV)	i_{corr} $(\mu A/cm^2)$	β_a (mV/decade)	$-\beta_c$ (mV/decade)	% IE
without inhibitor	-277	161.30	89.73	132.60	-
with 1000 rpm	-258	45.90	68.84	136.10	71.54

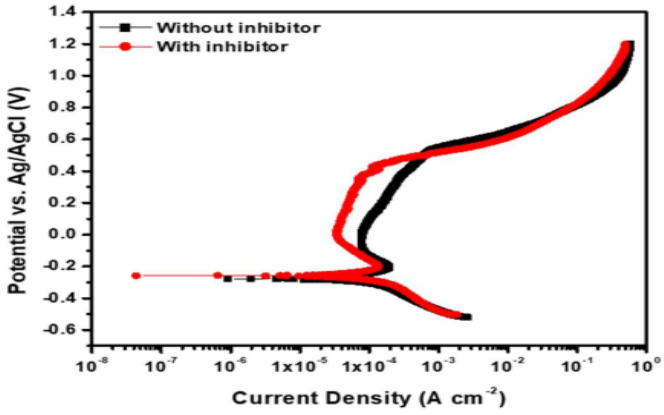

Figure 6: PDP plots for SS316L stainless steel during corrosion in 2 % HCl + 3.5 % NaCl without and with 1-benzylimidazole.

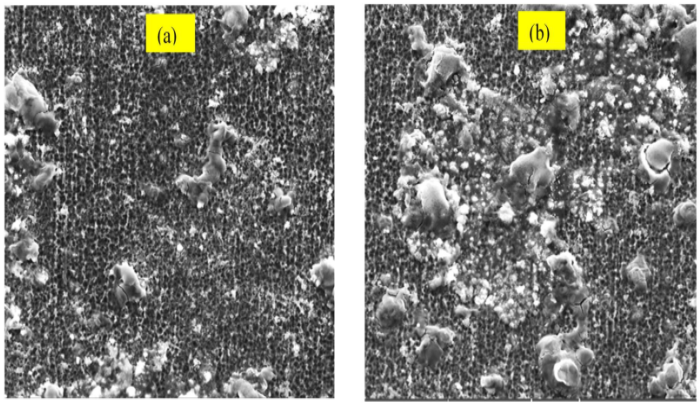

Figure 7: SEM surface morphology of SS316L stainless steel after polarization in 2 % HCl + 3.5 % NaCl (a) without and (b) with 1-benzylimidazole.

frequency) and at a corrosion layer-substrate interface (at low frequency) [25]. Compared with the single time constant for the uninhibited stainless steel, the two time constants in the presence of 1-benzylimidazole is due to the adsorbed corrosion inhibitor layer which isolates the stainless steel substrate from the acid solution. Consequently, the Figure 5d and 5e were adopted as electrical models to interpret the corrosion phenomena for the uninhibited and inhibited stainless steel, respectively, after fitting experimental results using the Echem Analysts software. The values of respective electrical elements are detailed in Table 2.

The elements R_s, R_{ct} and CPE_{dl} represent the solution resistance, charge transfer resistance and double layer capacitance, respectively. The use of constant phase element (CPE), rather than pure capacitor, in the model is to account for surface roughness of the corroding alloy [26]. The R_{ct} is equivalent to the corrosion resistance of the corroding metal while the CPE_{dl} elements, Y_{dl} and n, describe the admittance of charge into the double layer and the roughness of the alloy surface (α_{dl}), respectively. In Figure 5e, the characteristic of the adsorbed inhibitor layer is characterized by the R_f and CPE_f elements (Y_f and α_f) which, respectively, describe the porosity of the adsorbed layer and the charge capacitance at the layer-solution interface. From Table 2, the lower Y_{dl} values obtained in the presence of 1-benzylimidazole confirms that the inhibitor adsorption reduces the accumulation of corrosion-inducing aqueous species at the stainless steel surface and, thus, lowers the rate of charge transfer at the alloy surface-solution interface. As Table shows, the inhibitor adsorption impacts a total resistance ($R_{ct} + R_f$) of 765 Ωcm^2, compared with the value of 212 Ωcm^2 recorded for the blank solution. This gives an inhibition efficiency of 72.29 %, based on the Equation (7). Furthermore, the α_{dl} value is also higher in the presence of inhibitor, which indicates that the inhibitor adsorption minimizes the roughness of the alloy surface due to the corrosion attack.

$$\%IE_{EIS} = 1 - \frac{R_{\text{total(with inhibitor)}}}{R_{\text{total(without inhibitor)}}} \times 100\% \quad (7)$$

$$\%IE_{PDP} = 1 - \frac{i_{\text{corr(with inhibitor)}}}{i_{\text{corr(without inhibitor)}}} \times 100\% \quad (8)$$

In Figure 6, each PDP curve shows an activation-controlled cathodic arm representing the dominant H^+ reduction in the acid solution. The anodic arm is characterized by an active region, a region of passivation and a region of passivation breakdown. The active region is attributed to the oxidation and dissolution of surface elements like Fe and Cr, the passivation potential region depicts the formation of protective oxides and hydroxides of Fe and Cr [27], whereas the region of passivation breakdown indicates potential regions where protective passive layer is broken, especially locally by chloride ions.

Extrapolating the PDP plots around ± 10 mV of the cathodic-anodic potential transition enabled the deduction of corrosion current density (i_{corr}), corrosion potential (E_corr), anodic (β_a) and cathodic (β_c) Tafel constants [28]. The E corr indicates the thermodynamic tendency to corrode in the solution and the most preferable active sites of corrosion inhibitor interaction with the corroding surface, while the i_{corr} is a measure of the corrosion rate.

By Table 3, the presence of 1-benzylimidazole in the acid solution slightly shifts the E corr towards more anodic potential and lowers the i corr value from 161.30 μ A cm^{-2} to 45.90 $\mu A cm^{-2}$; which amounted to an inhibition efficiency of 71.54 % according to Equation (8). It is reported that 1-benzylimidazole exists as a cationic species in acidic solution [17]. Therefore, the greater inclination of 1-benzylimidazole to adsorb on anodic sites of the stainless steel strongly suggests the existence of pre-adsorbed anions on the anodic sites containing Fe^{2+} and Cr^{3+}, which eventually attract the cationic inhibitor towards the anode. Such phenomenon was also reported elsewhere for 1-benzylimidazole in CO_2 + H_2S-saturated NaCl solution [16]. This anodic preference is a stronger inclination towards more protective passivation, as confirmed by Figure 6; where the inhibitor shifts passivation current to lower values. Although the inhibitor does not affect the passivation potential (and passivation mechanism), it strongly modifies the passive film formed into a more protective one. This means that 1-benzylimidazole adsorption encourages the formation of Fe and Cr oxides and hydroxides. Nevertheless, the inhibitor appears not too protective once the passive film is deteriorated. This is feasible because the adsorbing inhibitor molecules and nucleating corrosion products would experience some structural mismatch which are easily targeted for localized attack and collapse.

3.4. SEM results

The surface morphologies of the stainless steel, after polarization in the acid solution without and with 1000 ppm of 1-benzylimidazole, are presented in Figure 7a and 7b, respectively. In the absence of inhibitor, Figure 7a, the stainless steel surface exhibits a rough morphology with patches of passive products around the surface. In the presence of inhibitor, Figure 7b, the passive products appear to agglomerate into a more continuous and denser layer which provides more surface coverage for the alloy surface. This justifies the findings from electrochemical measurements that the adsorption of 1- benzylimidazole could facilitate the formation of passive layer. At some points, however, some shallow cracks could be observed in the Figure 7b. These are likely points where localized corrosion occurs when the alloy is polarized beyond the passivation region.

4. Conclusion

The corrosion characteristics of a chemical reactor alloy SS316L stainless steel, and its inhibition by 1-benzylimidazole, have been investigated in 2 % HCl + 3.5 % NaCl solution (a typical solution used for industrial acid cleaning). The addition of 1-benzylimidazole into the test solution significantly lowered the rate of corrosion of the alloy, wherein an optimum inhibitor concentration of 1000 ppm yielded inhibition efficiency greater than 70 %. The 1-benzylimidazole acted more like an anodic-type inhibitor which improved the characteristics of the passive film formed on the alloy surface. The adsorption of 1-benzylimidazole followed the Temkin isotherm and protected the stainless steel surface from localized corrosion, based on SEM characterization.

References

[1] J. Beddoes, J.G. Parr, "Introduction to Stainless Steels", 3rd ed. (1999), ASM International, Materials Park, Ohio, USA.

[2] Z. Zeng, N. Sakoda, T. Tajiri, S. Kuroda, "Structure and corrosion behaviour of 316L stainless steel coatings formed by HVAF spraying with and without sealing", Surface and Coatings Technology **203** (2008) 284.

[3] I.B. Onyeachu, M.M. Solomon, "Benzotriazole derivative as an effective corrosion inhibitor for low carbon steel in 1 M HCl and 1 M HCl + 3.5wt.% NaCl solutions", Journal of Molecular Liquids **313** (2020) 113536.

[4] I.B. Obot, A. Meroufel, I.B. Onyeachu, A. Alenazi, A.A. Sorour, "Corrosion inhibitors for acid cleaning of desalination heat exchangers: Progress, challenges and future perspectives", Journal of Molecular Liquids **296** (2019) 111760.

[5] S.A. Thakur, G.P. Flake, G.S. Travlos, J.A. Dill, S.L. Grumbein, S.J. Harbo, M.J. Hooth, "Evaluation of propargyl alcohol toxicity and carcinogenicity in F344/N rats and B6C3F1/N mice following whole-body inhalation exposure". Toxicology **314** (2013) 100.

[6] W.H. Beggs, F.A. Andrews, G.A. Sarosi, "Action of imidazole-containing antifungal drugs", Life Sciences **28** (1981) 111.

[7] P. Lindberg, P. Nordberg, T. Alminger, A. Brandstorm, B. Wallmark, "The mechanism of action of the antisecretory agent omeprazole", Journal of Medicinal Chemistry **29** (1986) 1327.

[8] A. Singh, K.R. Ansari, A. Kumar, W. Liu, C. Songsong, Y. Lin, "Electrochemical, surface and quantum chemical studies of novel imidazole derivatives as corrosion inhibitors for J55 steel in sweet corrosive environment", Journal of Alloys and Compounds **712** (2017) 121.

[9] T. Yan, S. Zhang, L. Feng, Y. Qiang, L. Lu, D. Fu, B. Tan, "Investigation of imidazole derivatives as corrosion inhibitors of copper in sulfuric acid: combination of experimental and theoretical researches", Journal of the Taiwan Institute of Chemical Engineers **106** (2020) 118.

[10] M. Talari, S.M. Nezhad, S.J. Alavi, M. Mohtashamipour, A. Davoodi, S. Hosseinpour, "Experimental and computational chemistry studies of two imidazole-based compounds as corrosion inhibitors for mild steel in HCl solution", Journal of Molecular Liquids **286** (2019) 110915.

[11] J. Wang, D. Liu, S. Cao, S. Pan, H. Luo, T. Wang, H. Ding, B.B. Mamba, J. Gui, "Inhibition effect of monomeric/polymerized imidazole zwitterions as corrosion inhibitors for carbon steel in acid medium", Journal of Molecular Liquids **312** (2020) 113436.

[12] C. Cardona, A.A. Torres, J.M. Miranda-Vidales, J.T. Pérez, M.M. González-Chávez, H. Herrera- Hernández, L. Narváez, "Assessment of Dimethylbenzodiimidazole as Corrosion Inhibitor of Austenitic Stainless Steel Grade 316L in Acid Medium", Int. J. Electrochemical Science **10** (2015) 1966.

[13] M.T. Zaky, M.I. Nessim, M.A. Deyab, "Synthesis of new ionic liquids based on dicationic imidazolium and their anti-corrosion performances", Journal of Molecular Liquids **290** (2019) 111230.

[14] Paris Commission (PARCOM) (2006). Protocols on Methods for the Testing of Chemicals Used in the Offshore Oil Industry. Paris, France.

[15] 1-benzylimidazole, Material Safety Data Sheet, www.caymanchem.com/msdss/70510m.pdf (Retrieved 16 th January, 2022).

[16] I.B. Onyeachu, D.I. Njoku, S. Kaya, B. El Ibrahimi, C.F Nnadozie, "Sour corrosion of C1018 carbon steel and its inhibition by 1-benzylimidazole: electrochemical, SEM, FTIR and computational assessment", Adhesion Science and Technology (2021) 1. DOI: 10.1080/01694243.2021.1938474.

[17] A. Ismail, H.M. Irshad, A. Zeino, I.H. Toor, "Electrochemical corrosion performance of aromatic functionalized imidazole inhibitor under hydrodynamic conditions on API X65 carbon steel in 1M HCl Solution", Arabian Journal of Science and Engineering **44** (2019) 5877.

[18] H. Kumar, T. Dhanda, "Experimental and theoretical (MDS and FMO) study of 1-Benzylimidazole for mild steel in 0.1 N H 2 SO 4 at normal and elevated temperatures: An efficient anti-pitting and anti-cracking agent", Journal of Molecular Structure **1231** (2021) 129958.

[19] I.B. Obot, M.M. Solomon, I.B. Onyeachu, S.A. Umoren, A. Meroufel, A. Alenazi, A.A. Sorour, "Development of a green corrosion inhibitor for use in acid cleaning of MSF desalination plant", Desalination **495** (2020) 114675.

[20] ASTM-G 01-03, Standard practice for preparing, cleaning, and evaluation corrosion test specimens, ASTM Book of Standards (Re-approved 1997).

[21] I.B. Onyeachu, M.M. Solomon, S.A. Umoren, I.B. Obot, A.A. Sorour, "Corrosion inhibition effect of a benzimidazole derivative on heat exchange tubing materials during acid cleaning of multistage flash desalination plants", Desalination **479** (2020) 114283.

[22] C.C. Ahanotu, I.B. Onyeachu, M.M. Solomon, I.S. Chikwe, O.B. Chikwe, C.A. Eziukwu, "Pterocarpus santalinoides leaves extract as a sustainable and potent inhibitor for low carbon steel in a simulated pickling medium", Sustainable Chemistry and Pharmacy **15** (2020) 100196.

[23] O.A. Akinbulumo, O.J. Odejobi, E.L. Odekanle, "Thermodynamics and adsorption study of the corrosion inhibition of mild steel by Euphorbia heterophylla L. extract in 1.5 M HCl", Results Mater. **5** (2020) 100074.

[24] S. Chaudhary, R.K. Tak, "Natural corrosion inhibition and adsorption characteristics of Tribulus terrestris plant extract on aluminium in hydrochloric acid environment", Biointerface Research in Applied Chemistry **12** (2022) 2603.

[25] A. Espinoza-Vazquez, F.J. Rodriguez-Gomez, "Caffeine and nicotine in 3 % NaCl solution with CO_2 as corrosion inhibitors for low carbon steel", RSC Advances **6** (2016) 70226.

[26] C.H. Hsu, F. Mansfeld, "Technical note: concerning the conversion of the constant phase element parameter Y o into a capacitance", Corrosion **57** (2001) 747.

[27] H.H. Strehblow, "Passivity of metals studied by surface analytical methods, a review", Electrochimica Acta **212** (2016) 630.

[28] M. Stern, A.L. Geary, "Electrochemical polarization, 1. A theoretical analysis of the shape of polarization curves", The Electrochemical Society **104** (1957) 751.